Optics EXPRESS

Review on photonic properties of nanowires for photovoltaics [Invited]

S. MOKKAPATI* AND C. JAGADISH

Department of Electronic Materials Engineering, Research School of Physics and Engineering, The Australian National University, Canberra, A. C. T., 2601, Australia
**sudha.mokkapati@anu.edu.au*

Abstract: III-V semiconductor nanowires behave as optical antennae because of their shape anisotropy and high refractive index. The antennae like behavior modifies the absorption and emission properties of nanowires compared to planar materials. Nanowires absorb light more efficiently compared to an equivalent volume planar material, leading to higher short circuit current densities. The modified emission from the nanowires has the potential to increase the open circuit voltage from nanowire solar cells compared to planar solar cells. In order to achieve high efficiency nanowire solar cells it is essential to control the surface state density and doping in nanowires. We review the physics of nanowire solar cells and progress made in addressing the surface recombination and doping of nanowires, with emphasis on GaAs and InP materials.

OCIS codes: (350.6050) Solar energy; (160.4236) Nanomaterials; (160.6000) Semiconductor materials.

References and links

1. B. M. Kayes, H. A. Atwater, and N. S. Lewis, "Comparison of the device physics principles of planar and radial p-n junction nanorod solar cells," J. Appl. Phys. **97**(11), 114302 (2005).
2. J. Wallentin, N. Anttu, D. Asoli, M. Huffman, I. Åberg, M. H. Magnusson, G. Siefer, P. Fuss-Kailuweit, F. Dimroth, B. Witzigmann, H. Q. Xu, L. Samuelson, K. Deppert, and M. T. Borgström, "InP Nanowire Array Solar Cells Achieving 13.8% Efficiency by Exceeding the Ray Optics Limit," Science **339**(6123), 1057–1060 (2013).
3. I. Aberg, G. Vescovi, D. Asoli, U. Naseem, J. P. Gilboy, C. Sundvall, A. Dahlgren, K. E. Svensson, N. Anttu, M. T. Bjork, and L. Samuelson, "A GaAs Nanowire Array Solar Cell With 15.3% Efficiency at 1 Sun," IEEE J. Photovolt. **6**, 185–190 (2016).
4. P. Krogstrup, H. I. Jorgensen, M. Heiss, O. Demichel, J. V. Holm, M. Aagesen, J. Nygard, and I. Anna Fontcuberta, "Single-nanowire solar cells beyond the Shockley-Queisser limit," Nat. Photonics **7**(4), 306–310 (2013).
5. S. Sandhu, Z. Yu, and S. Fan, "Detailed Balance Analysis and Enhancement of Open-Circuit Voltage in Single-Nanowire Solar Cells," Nano Lett. **14**(2), 1011–1015 (2014).
6. Y. Wenas, *unpublished*.
7. R. Paniagua-Domínguez, G. Grzela, J. G. Rivas, and J. A. Sánchez-Gil, "Enhanced and directional emission of semiconductor nanowires tailored through leaky/guided modes," Nanoscale **5**(21), 10582–10590 (2013).
8. G. Grzela, R. Paniagua-Domínguez, T. Barten, D. van Dam, J. A. Sánchez-Gil, and J. G. Rivas, "Nanowire Antenna Absorption Probed with Time-Reversed Fourier Microscopy," Nano Lett. **14**(6), 3227–3234 (2014).
9. G. Grzela, R. Paniagua-Domínguez, T. Barten, Y. Fontana, J. A. Sánchez-Gil, and J. Gómez Rivas, "Nanowire Antenna Emission," Nano Lett. **12**(11), 5481–5486 (2012).
10. K. Okamoto, *Fundamentals of Optical Waveguides*, Second ed. (Elsevier Inc., 2006).
11. A. W. Snyder and J. D. Love, *Optical Waveguide Theory* (Kluwer Academic Publishers, 1983).
12. L. Cao, J. S. White, J.-S. Park, J. A. Schuller, B. M. Clemens, and M. L. Brongersma, "Engineering light absorption in semiconductor nanowire devices," Nat. Mater. **8**(8), 643–647 (2009).
13. Y. Yu and L. Cao, "Leaky mode engineering: A general design principle for dielectric optical antenna solar absorbers," Opt. Commun. **314**, 79–85 (2014).
14. A. Yariv, "Universal relations for coupling of optical power between microresonators and dielectric waveguides," Electron. Lett. **36**(4), 321–322 (2000).
15. C. F. Bohren and D. R. Huffman, *Absorption and Scattering of Light by Small Particles (*Wiley-VCH Verlag GmbH & Co. KGaA, 2004).
16. S. Mokkapati, D. Saxena, H. H. Tan, and C. Jagadish, "Optical design of nanowire absorbers for wavelength selective photodetectors," Sci. Rep. **5**, 15339 (2015).
17. S.-K. Kim, X. Zhang, D. J. Hill, K.-D. Song, J.-S. Park, H.-G. Park, and J. F. Cahoon, "Doubling Absorption in Nanowire Solar Cells with Dielectric Shell Optical Antennas," Nano Lett. **15**(1), 753–758 (2015).

#264987 http://dx.doi.org/10.1364/OE.24.017345
Journal © 2016 Received 11 May 2016; revised 17 Jul 2016; accepted 18 Jul 2016; published 22 Jul 2016
Corrected: 30 August 2016

Optics EXPRESS

18. M. D. Kelzenberg, S. W. Boettcher, J. A. Petykiewicz, D. B. Turner-Evans, M. C. Putnam, E. L. Warren, J. M. Spurgeon, R. M. Briggs, N. S. Lewis, and H. A. Atwater, "Enhanced absorption and carrier collection in Si wire arrays for photovoltaic applications," Nat. Mater. **9**(3), 239–244 (2010).
19. W. Shockley and H. J. Queisser, "Detailed Balance Limit of Efficiency of p-n Junction Solar Cells," J. Appl. Phys. **32**(3), 510–519 (1961).
20. P. Wurfel, *Physics of Solar Cells: From Basic Principles to Advanced* Concepts (Weinheim: Wiley-VCH, 2010).
21. T. Markvart, "Thermodynamics of losses in photovoltaic conversion," Appl. Phys. Lett. **91**(6), 064102 (2007).
22. U. Rau, U. W. Paetzold, and T. Kirchartz, "Thermodynamics of light management in photovoltaic devices," Phys. Rev. B **90**(3), 035211 (2014).
23. L. C. Hirst and N. J. Ekins-Daukes, "Fundamental losses in solar cells," Prog. Photovolt. Res. Appl. **19**(3), 286–293 (2011).
24. A. Polman and H. A. Atwater, "Photonic design principles for ultrahigh-efficiency photovoltaics," Nat. Mater. **11**(3), 174–177 (2012).
25. G. L. Araújo and A. Martí, "Absolute limiting efficiencies for photovoltaic energy conversion," Sol. Energ. Mat. and Sol. **33**(2), 213–240 (1994).
26. P. Campbell and M. A. Green, "The limiting efficiency of silicon solar cells under concentrated sunlight," IEEE Trans. Electron Dev. **33**(2), 234–239 (1986).
27. A. Martí, J. L. Balenzategui, and R. F. Reyna, "Photon recycling and Shockley's diode equation," J. Appl. Phys. **82**(8), 4067–4075 (1997).
28. A. Braun, E. A. Katz, D. Feuermann, B. M. Kayes, and J. M. Gordon, "Photovoltaic performance enhancement by external recycling of photon emission," Energy Environ. Sci. **6**(5), 1499–1503 (2013).
29. E. D. Kosten, B. M. Kayes, and H. A. Atwater, "Experimental demonstration of enhanced photon recycling in angle-restricted GaAs solar cells," Energy Environ. Sci. **7**(6), 1907–1912 (2014).
30. O. D. Miller, E. Yablonovitch, and S. R. Kurtz, "Strong Internal and External Luminescence as Solar Cells Approach the Shockley&Queisser Limit," IEEE J. Photovolt. **2**(3), 303–311 (2012).
31. G. Grzela, D. Hourlier, and J. Gómez Rivas, "Polarization-dependent light extinction in ensembles of polydisperse vertical semiconductor nanowires: A Mie scattering effective medium," Phys. Rev. B **86**(4), 045305 (2012).
32. N. Anttu, "Shockley–Queisser Detailed Balance Efficiency Limit for Nanowire Solar Cells," ACS Photonics **2**(3), 446–453 (2015).
33. J. Claudon, J. Bleuse, N. S. Malik, M. Bazin, P. Jaffrennou, N. Gregersen, *et al*., "A highly efficient single-photon source based on a quantum dot in a photonic nanowire," Nat. Photonics **4**, 174–177 (2010).
34. M. E. Reimer, G. Bulgarini, N. Akopian, M. Hocevar, M. B. Bavinck, M. A. Verheijen, E. P. A. M. Bakkers, L. P. Kouwenhoven, and V. Zwiller, "Bright single-photon sources in bottom-up tailored nanowires," Nat. Commun. **3**, 737 (2012).
35. G. Bulgarini, M. E. Reimer, M. Bouwes Bavinck, K. D. Jöns, D. Dalacu, P. J. Poole, E. P. A. M. Bakkers, and V. Zwiller, "Nanowire Waveguides Launching Single Photons in a Gaussian Mode for Ideal Fiber Coupling," Nano Lett. **14**(7), 4102–4106 (2014).
36. N. Anttu, "Shockley–Queisser Detailed Balance Efficiency Limit for Nanowire Solar Cells," ACS Photonics **2**(3), 446–453 (2015).
37. Y. Xu, T. Gong, and J. N. Munday, "The generalized Shockley-Queisser limit for nanostructured solar cells," Sci. Rep. **5**, 13536 (2015).
38. K. R. Catchpole, S. Mokkapati, and F. J. Beck, "Comparing nanowire, multijunction, and single junction solar cells in the presence of light trapping," J. Appl. Phys. **109**(8), 084519 (2011).
39. R. R. LaPierre, "Numerical model of current-voltage characteristics and efficiency of GaAs nanowire solar cells," J. Appl. Phys. **109**(3), 034311 (2011).
40. Z. Li, Y. C. Wenas, L. Fu, S. Mokkapati, H. H. Tan, and C. Jagadish, "Influence of Electrical Design on Core Shell GaAs Nanowire Array Solar Cells," IEEE J Photovolt. **5**(3), 854–864 (2015).
41. A. C. E. Chia and R. R. LaPierre, "Analytical model of surface depletion in GaAs nanowires," J. Appl. Phys. **112**(6), 063705 (2012).
42. R. Calarco, M. Marso, T. Richter, A. I. Aykanat, R. Meijers, A. V D Hart, T. Stoica, and H. Lüth, "Size-dependent Photoconductivity in MBE-Grown GaN-Nanowires," Nano Lett. **5**(5), 981–984 (2005).
43. O. Demichel, M. Heiss, J. Bleuse, H. Mariette, and A. Fontcuberta i Morral, "Impact of surfaces on the optical properties of GaAs nanowires," Appl. Phys. Lett. **97**(20), 201907 (2010).
44. C.-C. Chang, C.-Y. Chi, M. Yao, N. Huang, C.-C. Chen, J. Theiss, A. W. Bushmaker, S. Lalumondiere, T. W. Yeh, M. L. Povinelli, C. Zhou, P. D. Dapkus, and S. B. Cronin, "Electrical and Optical Characterization of Surface Passivation in GaAs Nanowires," Nano Lett. **12**(9), 4484–4489 (2012).
45. S. Thunich, L. Prechtel, D. Spirkoska, G. Abstreiter, A. Fontcuberta i Morral, and A. W. Holleitner, "Photocurrent and photoconductance properties of a GaAs nanowire," Appl. Phys. Lett. **95**(8), 083111 (2009).
46. H. J. Joyce, C. J. Docherty, Q. Gao, H. H. Tan, C. Jagadish, J. Lloyd-Hughes, L. M. Herz, and M. B. Johnston, "Electronic properties of GaAs, InAs and InP nanowires studied by terahertz spectroscopy," Nanotechnology **24**(21), 214006 (2013).
47. H. J. Joyce, J. Wong-Leung, C.-K. Yong, C. J. Docherty, S. Paiman, Q. Gao, H. H. Tan, C. Jagadish, J. Lloyd-Hughes, L. M. Herz, and M. B. Johnston, "Ultralow Surface Recombination Velocity in InP Nanowires Probed by Terahertz Spectroscopy," Nano Lett. **12**(10), 5325–5330 (2012).

48. B. J. Skromme, C. J. Sandroff, E. Yablonovitch, and T. Gmitter, "Effects of passivating ionic films on the photoluminescence properties of GaAs," Appl. Phys. Lett. **51**(24), 2022–2024 (1987).
49. C. J. Sandroff, R. N. Nottenburg, J. C. Bischoff, and R. Bhat, "Dramatic enhancement in the gain of a GaAs/AlGaAs heterostructure bipolar transistor by surface chemical passivation," Appl. Phys. Lett. **51**(1), 33–35 (1987).
50. A. Lin, J. N. Shapiro, P. N. Senanayake, A. C. Scofield, P. S. Wong, B. Liang, and D. L. Huffaker, "Extracting transport parameters in GaAs nanopillars grown by selective-area epitaxy," Nanotechnology **23**(10), 105701 (2012).
51. M. T. Sheldon, C. N. Eisler, and H. A. Atwater, "GaAs Passivation with Trioctylphosphine Sulfide for Enhanced Solar Cell Efficiency and Durability," Adv. Energy Mater. **2**(3), 339–344 (2012).
52. J. Lloyd-Hughes, S. K. E. Merchant, L. Fu, H. H. Tan, C. Jagadish, E. Castro-Camus, and M. B. Johnston, "Influence of surface passivation on ultrafast carrier dynamics and terahertz radiation generation in GaAs," Appl. Phys. Lett. **89**(23), 232102 (2006).
53. N. Tajik, Z. Peng, P. Kuyanov, and R. R. LaPierre, "Sulfur passivation and contact methods for GaAs nanowire solar cells," Nanotechnology **22**(22), 225402 (2011).
54. V. L. Berkovits, D. Paget, A. N. Karpenko, V. P. Ulin, and O. E. Tereshchenko, "Soft nitridation of GaAs(100) by hydrazine sulfide solutions: Effect on surface recombination and surface barrier," Appl. Phys. Lett. **90**(2), 022104 (2007).
55. P. A. Alekseev, M. S. Dunaevskiy, V. P. Ulin, T. V. Lvova, D. O. Filatov, A. V. Nezhdanov, A. I. Mashin, and V. L. Berkovits, "Nitride Surface Passivation of GaAs Nanowires: Impact on Surface State Density," Nano Lett. **15**(1), 63–68 (2015).
56. L. K. van Vugt, S. J. Veen, E. P. A. M. Bakkers, A. L. Roest, and D. Vanmaekelbergh, "Increase of the Photoluminescence Intensity of InP Nanowires by Photoassisted Surface Passivation," J. Am. Chem. Soc. **127**(35), 12357–12362 (2005).
57. N. Tajik, A. C. E. Chia, and R. R. LaPierre, "Improved conductivity and long-term stability of sulfur-passivated n-GaAs nanowires," Appl. Phys. Lett. **100**(20), 203122 (2012).
58. R. J. Nelson and R. G. Sobers, "Interfacial recombination velocity in GaAlAs/GaAs heterostructures," Appl. Phys. Lett. **32**(11), 761–763 (1978).
59. S. Perera, M. A. Fickenscher, H. E. Jackson, L. M. Smith, J. M. Yarrison-Rice, H. J. Joyce, Q. Gao, H. H. Tan, C. Jagadish, X. Zhang, and J. Zou, "Nearly intrinsic exciton lifetimes in single twin-free GaAs/AlGaAs core-shell nanowire heterostructures," Appl. Phys. Lett. **93**(5), 053110 (2008).
60. P. Parkinson, H. J. Joyce, Q. Gao, H. H. Tan, X. Zhang, J. Zou, C. Jagadish, L. M. Herz, and M. B. Johnston, "Carrier Lifetime and Mobility Enhancement in Nearly Defect-Free Core-Shell Nanowires Measured Using Time-Resolved Terahertz Spectroscopy," Nano Lett. **9**(9), 3349–3353 (2009).
61. L. Ouattara, A. Mikkelsen, N. Sköld, J. Eriksson, T. Knaapen, E. Ćavar, W. Seifert, L. Samuelson, and E. Lundgren, "GaAs/AlGaAs Nanowire Heterostructures Studied by Scanning Tunneling Microscopy," Nano Lett. **7**(9), 2859–2864 (2007).
62. N. Sköld, L. S. Karlsson, M. W. Larsson, M.-E. Pistol, W. Seifert, J. Trägårdh, and L. Samuelson, "Growth and Optical Properties of Strained GaAs-Ga_xIn_{1-x} P Core-Shell Nanowires," Nano Lett. **5**(10), 1943–1947 (2005).
63. G. Mariani, A. C. Scofield, C.-H. Hung, and D. L. Huffaker, "GaAs nanopillar-array solar cells employing in situ surface passivation," Nat. Commun. **4**, 1497 (2013).
64. T. Haggren, H. Jiang, J.-P. Kakko, T. Huhtio, V. Dhaka, E. Kauppinen, and H. Lipsanen, "Strong surface passivation of GaAs nanowires with ultrathin InP and GaP capping layers," Appl. Phys. Lett. **105**(3), 033114 (2014).
65. K. Haraguchi, T. Katsuyama, K. Hiruma, and K. Ogawa, "GaAs p-n junction formed in quantum wire crystals," Appl. Phys. Lett. **60**(6), 745–747 (1992).
66. E. Dimakis, M. Ramsteiner, A. Tahraoui, H. Riechert, and L. Geelhaar, "A. tahraoui, H. Riechert, and L. Geelhaar, "Shell-doping of GaAs nanowires with Si for n-type conductivity," Nano Res. **5**(11), 796–804 (2012).
67. C. Gutsche, A. Lysov, I. Regolin, K. Blekker, W. Prost, and F.-J. Tegude, "n-Type Doping of Vapor–Liquid–Solid Grown GaAs Nanowires," Nanoscale Res. Lett. **6**, 65 (2011).
68. H. G. Lee, H. C. Jeon, T. W. Kang, and T. W. Kim, "Gallium arsenide crystalline nanorods grown by molecular-beam epitaxy," Appl. Phys. Lett. **78**(21), 3319–3321 (2001).
69. M. Hilse, M. Ramsteiner, S. Breuer, L. Geelhaar, and H. Riechert, "Incorporation of the dopants Si and Be into GaAs nanowires," Appl. Phys. Lett. **96**(19), 193104 (2010).
70. J. A. Czaban, D. A. Thompson, and R. R. LaPierre, "GaAs Core-Shell Nanowires for Photovoltaic Applications," Nano Lett. **9**(1), 148–154 (2009).
71. J. Caram, C. Sandoval, M. Tirado, D. Comedi, J. Czaban, D. A. Thompson, and R. R. LaPierre, "Electrical characteristics of core-shell p-n GaAs nanowire structures with Te as the n-dopant," Nanotechnology **21**(13), 134007 (2010).
72. K. Tomioka, J. Motohisa, S. Hara, K. Hiruma, and T. Fukui, "GaAs/AlGaAs Core Multishell Nanowire-Based Light-Emitting Diodes on Si," Nano Lett. **10**(5), 1639–1644 (2010).
73. X. Duan, Y. Huang, Y. Cui, J. Wang, and C. M. Lieber, "Indium phosphide nanowires as building blocks for nanoscale electronic and optoelectronic devices," Nature **409**(6816), 66–69 (2001).
74. C. Gutsche, I. Regolin, K. Blekker, A. Lysov, W. Prost, and F. J. Tegude, "Controllable p-type doping of GaAs nanowires during vapor-liquid-solid growth," J. Appl. Phys. **105**(2), 024305 (2009).

75. O. Salehzadeh, X. Zhang, B. D. Gates, K. L. Kavanagh, and S. P. Watkins, "p-type doping of GaAs nanowires using carbon," J. Appl. Phys. **112**(9), 094323 (2012).
76. J. Wallentin, J. M. Persson, J. B. Wagner, L. Samuelson, K. Deppert, and M. T. Borgström, "High-Performance Single Nanowire Tunnel Diodes," Nano Lett. **10**(3), 974–979 (2010).
77. C. Liu, L. Dai, L. P. You, W. J. Xu, and G. G. Qin, "Blueshift of electroluminescence from single n-InP nanowire/p-Si heterojunctions due to the Burstein-Moss effect," Nanotechnology **19**(46), 465203 (2008).
78. M. H. M. van Weert, O. Wunnicke, A. L. Roest, T. J. Eijkemans, A. Yu Silov, J. E. M. Haverkort, G. W. 't Hooft, and E. P. A. M. Bakkers, "Large redshift in photoluminescence of p-doped InP nanowires induced by Fermi-level pinning," Appl. Phys. Lett. **88**(4), 043109 (2006).
79. J. Wallentin, M. Ek, L. R. Wallenberg, L. Samuelson, K. Deppert, and M. T. Borgström, "Changes in Contact Angle of Seed Particle Correlated with Increased Zincblende Formation in Doped InP Nanowires," Nano Lett. **10**(12), 4807–4812 (2010).
80. C. Colombo, M. Heiß, M. Grätzel, and A. Fontcuberta i Morral, "Gallium arsenide p-i-n radial structures for photovoltaic applications," Appl. Phys. Lett. **94**(17), 173108 (2009).
81. B. Ketterer, E. Mikheev, E. Uccelli, and A. Fontcuberta i Morral, "Compensation mechanism in silicon-doped gallium arsenide nanowires," Appl. Phys. Lett. **97**(22), 223103 (2010).
82. J. Dufouleur, C. Colombo, T. Garma, B. Ketterer, E. Uccelli, M. Nicotra, A. Fontcuberta i Morral, and I. Morral, "P-Doping Mechanisms in Catalyst-Free Gallium Arsenide Nanowires," Nano Lett. **10**(5), 1734–1740 (2010).
83. B. Ketterer, E. Uccelli, and A. Fontcuberta i Morral, "Mobility and carrier density in p-type GaAs nanowires measured by transmission Raman spectroscopy," Nanoscale **4**(5), 1789–1793 (2012).
84. M. Zervos, "Delta(δ)-doping of semiconductor nanowires," Phys. Status Solidi Rapid Res. Lett. **7**(9), 651–654 (2013).
85. J. L. Boland, S. Conesa-Boj, P. Parkinson, G. Tütüncüoglu, F. Matteini, D. Rüffer, A. Casadei, F. Amaduzzi, F. Jabeen, C. L. Davies, H. J. Joyce, L. M. Herz, A. Fontcuberta i Morral, and M. B. Johnston, "Modulation Doping of GaAs/AlGaAs Core-Shell Nanowires with Effective Defect Passivation and High Electron Mobility," Nano Lett. **15**(2), 1336–1342 (2015).
86. D. Spirkoska, A. Fontcuberta i Morral, J. Dufouleur, Q. Xie, and G. Abstreiter, "Free standing modulation doped core–shell GaAs/AlGaAs hetero-nanowires," Phys. Status Solidi Rapid Res. Lett. **5**(9), 353–355 (2011).
87. K. Sladek, V. Klinger, J. Wensorra, M. Akabori, H. Hardtdegen, and D. Grützmacher, "MOVPE of n-doped GaAs and modulation doped GaAs/AlGaAs nanowires," J. Cryst. Growth **312**(5), 635–640 (2010).

1. Introduction

One of the requirements to achieve high efficiency in solar cells is the ability to maintain large optical thickness to facilitate efficient light absorption and small electrical thickness to facilitate efficient photogenerated carrier collection at the contacts. 'Light trapping' is conventionally used to decouple the optical and electrical thickness of solar cells, thereby enabling solar cells with low quality absorbers (materials with small minority carrier diffusion length). Semiconductor nanowires are anisotropic structures with base dimensions of the order of few 10-100 nms and longitudinal dimensions of the order of few microns. The shape anisotropy of nanowires provides opportunities to decouple the optical and electrical thickness of solar cells. Seminal work by Kayes et. al. [1] that proposed the design of radial junction nanowire solar cells, where the longitudinal dimensions and lateral dimensions of nanowires determine the optical and electrical thickness of a nanowire solar cell sparked huge interest in the research of nanowire solar cells. Since then, there have been a lot of publications, both theoretical and experimental, discussing and demonstrating various aspects of nanowire solar cells.

While nanowires of any semiconducting material offer above advantages for solar cells, III-V compound semiconductors like GaAs and InP are especially promising for photovoltaics because of their direct bandgaps, close to the ideal value for maximizing power conversion efficiency under AM 1.5 G spectrum. Highest efficiency of 13.8% and 15.3% has been demonstrated for InP [2] and GaAs [3] nanowire array solar cells under 1 sun illumination. While these efficiencies look promising, they are significantly lower than the theoretical maximum efficiencies that can be achieved in nanowire solar cells. We review the understanding developed on nanowire solar cells, with regards to maximum short circuit current density, J_{sc}, and open circuit voltage, V_{oc}, in the context of single nanowires with illumination either parallel or perpendicular to the nanowire axis and nanowire arrays. While the theoretical concepts discussed in the manuscript are applicable to any semiconductor material, we review the challenges limiting the nanowire solar cell efficiencies with emphasis on III-V compound semiconductors, in particular GaAs and InP.

2. Currents in a nanowire solar cell

III-V semiconductor nanowires, despite their small cross-section dimensions, exhibit strong waveguiding properties for light with energy close to or less than the bandgap energy of the semiconductor because of high refractive index of the semiconductor in this energy range. For this reason, compound semiconductor nanowires behave as optical antennae: (i) they have the ability to concentrate incident light [4–6] and (ii) they have directional emission and absorption properties [7–9]. The ability of the nanowires to concentrate incident light enables efficient (near perfect) light absorption in small volume material [2–6]. Reducing the semiconductor volume required for efficient light absorption is an important criteria for lowering the materials costs associated with solar cells. We will discuss the light concentration ability of nanowires in this section, and the directional light emission properties of nanowires in the context of V_{oc} (Section 3).

Firstly, we give a brief description of the waveguiding properties of semiconductor nanowires. Considering nanowires as cylinders with uniform cross section dimensions, and solving Maxwell's equations with appropriate boundary conditions [10,11] yields Eigen modes of two different kinds for the nanowires. One class of solutions have the Poynting vector or power flow in the plane of the nanowire cross section (x-y plane) and are known as the whispering gallery modes or the leaky modes [Fig. 1(a)]. These modes are also described by the Mie theory. The second class of solutions have Poynting vector (power flow) along the nanowire axis (z-axis), and are known as the conventional waveguide modes [Fig. 1(b)].

The light incident on the nanowires can couple to the resonant modes supported in the nanowire. This provides an opportunity to engineer the light absorption in nanowires by controlling their physical dimensions. When the resonant modes supported in the nanowires are leaky, the overlap between the incident electromagnetic field and the guided mode profile is maximized, facilitating efficient coupling with incident light. The absorption properties of a horizontal nanowire [Fig. 1(c)] are determined by leaky-mode resonances or the Mie resonances supported in the nanowire [12] and the absorption properties of a vertical nanowire [Fig. 1(d)] are determined by the conventional waveguide modes [6].

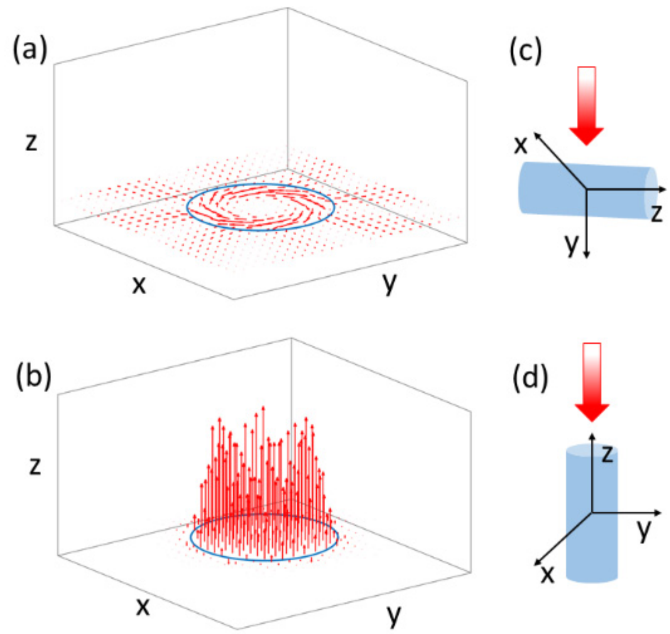

Fig. 1. (a) Poynting vector or direction of power flow for whispering gallery modes. The power flow is in the x-y plane or in a plane perpendicular to the nanowire axis. (b) Poynting vector or direction of power flow for conventional waveguide modes. The power flow is along the axis of the nanowire – z axis. (c), (d) the two illumination configurations discussed in the manuscript: (c) is the horizontal illumination configuration where light is incident on the nanowire in a direction perpendicular to its axis. (d) represents the vertical illumination configuration where light is incident on the nanowire in a direction parallel to its axis.

The absorption in the nanowire (in either vertical or horizontal illumination configuration), and hence the maximum current generated in a nanowire solar cell depends on the density of the corresponding resonant modes supported over the solar spectrum and their effective indices [13]. The absorption associated with a resonant mode in the nanowire is given by

$$P = \int C_{abs}(\lambda) I(\lambda) d\lambda \tag{1}$$

Where $I(\lambda)$ is the photon flux in the solar spectrum, $C_{abs}(\lambda)$ is the absorption cross-section of the nanowire and the integration is over the entire solar spectrum. The absorption associated with the resonant mode is maximized when the radiative loss of the mode is tuned to match the intrinsic absorption loss of the material of the nanowire, leading to 'critical coupling' between the incident solar spectrum and the resonant mode of the nanowire [13,14]. The total absorption is given by the sum of product of mode density and absorption associated with the corresponding resonant mode at each wavelength in the solar spectrum. Thus increasing the density of resonant modes supported in the nanowires over the solar spectrum will maximize absorption in the nanowire [5].

Numerical methods such as Finite Difference Time Domain (FDTD) or Rigorous Coupled Wave Theory (RCWA) are widely used to determine the absorption properties of nanowires. However, absorption resulting from Mie resonances can also be analytically modelled [5,15]. Because of the Mie resonances supported in a nanowire and efficient coupling of incident light to these resonances, the absorption in a horizontal nanowire is enhanced compared to a planar semiconductor of equivalent volume [5]. Likewise, for a vertical nanowire the absorption is enhanced compared to a planar semiconductor of equivalent volume because of

Optics EXPRESS

efficient coupling of incident light into conventional waveguide modes [6]. One of the advantages of using nanowires for solar cells is thus, the ability to generate similar currents using smaller volumes of semiconductors. For both vertical and horizontal illumination configurations, the maximum short circuit current density, J_{sc} that can be generated from the nanowire solar cell depends on the physical dimensions of the nanowire and shows oscillations with nanowire diameter [5,6]. The oscillations in J_{sc} for a horizontal InP nanowire are shown in Fig. 2 and are a consequence of waveguiding properties of the nanowires. This behavior is contrary to what is seen for a planar solar cell. For a planar solar cell, the current density initially increases with the thickness of the absorber and saturates at the maximum value represented by the dashed horizontal line in Fig. 2.

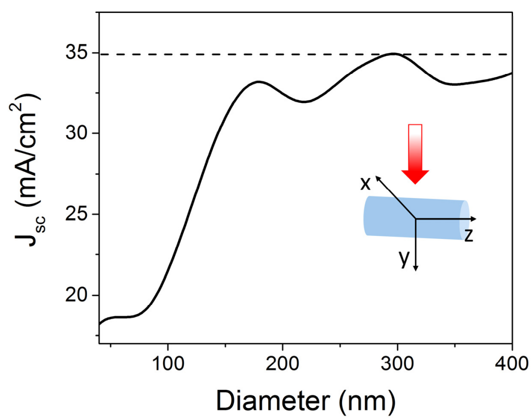

Fig. 2. Oscillations in numerically evaluated J_{sc} for an InP nanowire, as a function of the nanowire diameter. The horizontal dashed line represents the theoretical limit for J_{sc} for a planar InP solar cell. The inset represents the illumination configuration for the nanowire solar cell.

The absorption properties of nanowires can be modified/improved further by use of conformal dielectric shells around the nanowires. Low refractive index dielectric shells around the nanowire affect the density and spectral position of resonant modes supported in a nanowire. The dielectric shells also change the radiative loss associated with the resonant modes, and hence influence the in-coupling of incident light into the nanowires and its absorption properties [13,16]. Increase in short circuit current density of a nanowire solar cell has been experimentally achieved by conformally coating the nanowire with a dielectric shell [17]. Thus thickness and refractive index of dielectric shells around the nanowire can be used as an additional degree of freedom to engineer the absorption properties of nanowires.

Early demonstrations that nanowire arrays with very small filling fraction (~5%) can achieve similar absorption as in an equivalent thickness Si layer with Lambertian (~4n^2) path length enhancement [18] suggest that the absorption in a nanowire array is also dominated by the waveguiding properties of individual nanowires in the array, rather than the collective photonic crystal like behavior of the array. Studies on optimizing or maximizing the absorption in nanowire arrays also suggest that the behavior of the nanowire array can be modelled using a single nanowire [13], if the separation between adjacent nanowires is comparable to or larger than the size of the nanowires.

Optics EXPRESS

3. Open circuit voltage in a nanowire solar cell

In this section, we will discuss the maximum open circuit voltage, V_{oc} achievable in a nanowire solar cell. This value can be calculated using the detailed balance approach [5,6,19].The detailed balance analysis is based on balancing or equating the incoming photon flux to the sum of outgoing photon flux and particle flux at open circuit condition. Assuming perfect material quality and no non-radiative recombination,

$$F_s + F_{co} = F_c(V) + \frac{I}{q} \tag{2}$$

where F_s and F_{co} are the carrier generation rates in the solar cell due to incident solar photons and the surrounding black body radiation at solar cell ambient temperature, T_c, respectively, $F_c(V)$ is the bias-dependent radiative recombination rate and $\frac{I}{q}$ is the carrier extraction rate from the solar cell as external current, I.

F_s and F_{co} are given by

$$F_s = \frac{1}{hc}\int_0^{\lambda_g} \lambda I(\lambda) C_{abs}(\lambda,\theta,\phi) d\lambda \tag{3}$$

$$F_{co} = \int_0^{2\pi} d\phi \int_0^{\pi}\int_0^{\lambda_g} b(\lambda,T_c) C_{abs}(\lambda,\theta,\varphi) \sin\theta d\lambda d\theta \tag{4}$$

where $I(\lambda)$ is the AM1.5 solar spectral irradiance, $C_{abs}(\lambda,\theta,\phi)$ is the absorption cross-section of the solar cell corresponding to the angle of incidence defined by the polar angle θ and azimuthal angle ϕ, λ_g is the bandgap wavelength of the absorber, h is the Plank's constant, c is the velocity of light and $b(\lambda,T_c)$ is black-body radiation [20] at temperature T_c calculated using Plank's law. $F_c(V)$ is given by [5,6,19]:

$$F_c(V) = F_{co} \exp\left(\frac{qV}{K_b T_c}\right) \tag{5}$$

where k_b is the Boltzmann constant and V is the applied voltage.

The open circuit voltage, V_{oc}, can be determined from Eq. (2) by setting $I = 0$:

$$V_{oc} = \frac{K_b T_c}{q} \ln\left(\frac{F_s + F_{co}}{F_{co}}\right) \tag{6}$$

The absorption cross-section, $C_{abs}(\lambda,\theta,\phi)$, for a planar solar cell is defined as the product of the absorption coefficient of the absorber and the illumination area of the solar cell. $C_{abs}(\lambda,\theta,\phi)$ can be calculated analytically [15] for a horizontal nanowire and numerically determined for a vertical nanowire [6]. The V_{oc} for nanowires in both configurations exceeds that of a planar solar cell [5,6]. Interestingly, similar to J_{sc}, the V_{oc} shows oscillations with increasing nanowire diameter as shown in Fig. 3 for a horizontal InP nanowire, and is also a consequence of waveguided/leaky modes supported in the nanowire [5,6]. The inbuilt light concentration in nanowires due to efficient coupling of incident light into waveguided modes is equivalent to increasing the light generated current without affecting the reverse saturation current, and hence leads to an increase in V_{oc}.

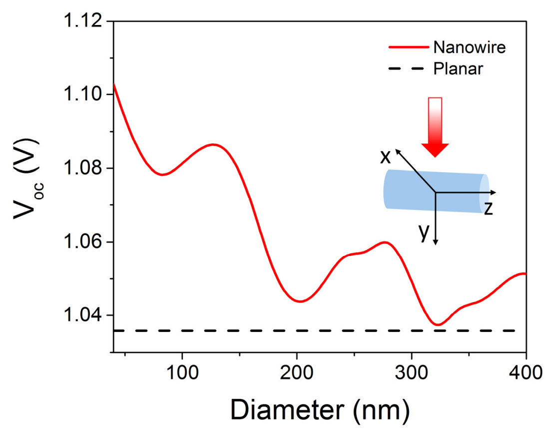

Fig. 3. Limiting value for the open circuit voltage achievable in a planar InP solar cell and a horizontal InP nanowire solar cell. Inset shows the nanowire illumination configuration.

The upper limit for the open circuit voltage of a solar cell can also be evaluated using a thermodynamics approach [21–23], and gives an alternative perspective on understanding the behavior of nanowire solar cells. The upper limit for the open circuit voltage, V_{oc} of a solar cell is determined by the Carnot's efficiency and the additional entropic losses that include thermalization loss, Etendue expansion loss and nonradiative loss [Eq. (7)].

$$qV_{oc} = E\left[1-\frac{T_c}{T_s}\right]+k_bT_c\ln\left[\frac{T_c}{T_s}\right]-k_bT_c\ln\left[\frac{\Omega_{em}}{\Omega_{sun}}\right]+\ln\left[QE\right] \tag{7}$$

where q is the charge of an electron, T_c and T_s are the temperature of the solar cell and the sun, respectively, k_b is the Boltzmann constant, Ω_{sun} is the solid angle for absorption, Ω_{em} is the solid angle for emission and QE is the quantum efficiency or radiative efficiency of the absorber. The first term on the right of Eq. (7) represents loss associated with conversion of photon energy into electrical energy in accordance with the Carnot's theorem, the second term represents the entropy losses due to thermal energy of carriers in the absorber. The third term is the voltage loss due to mismatch between the absorption (Ω_{sun}) and emission (Ω_{em}) solid angles and the last term represents the loss associated with non-radiative recombination in the absorber and hence is related to its optoelectronic quality.

The spontaneous emission from a conventional, bulk, planar solar cell is emitted into a solid angle of $\Omega_{em} = 4\pi$ sr, but the incoming light is incident within $\Omega_{sun} = 6\times10^{-5}$ sr [24]. This mismatch between the absorption and emission solid angles may lead to V_{oc} reduction of ~300 mV. A significant gain in the V_{oc} of a solar cell can be obtained by restricting the directionality of emission from the solar cell [25–27]. High V_{oc} has been achieved in case of planar solar cells by restricting the solid angle for light emission from GaAs solar cells using different approaches [28–30].

As discussed earlier, because of the waveguiding properties of III-V semiconductor nanowires, they behave as antennae and hence exhibit directional absorption and emission properties. The nanowire antennae behavior has been experimentally studied using the

Optics EXPRESS

Fourier imaging technique [7,9,31]. The ability to restrict the solid angle of spontaneous emission in nanowires by exploiting their waveguiding properties is promising to increase the V_{oc} achievable in nanowire solar cells by reducing the entropic losses associated with mismatch between solid angle for absorption and emission in a solar cell (third term on the right in Eq. (7). For optimal parameters, spontaneous emission from nanowire arrays is also anisotropic. Emission into the high index substrate is reduced compared to a planar semiconductor [32]. Enhanced, directional light extraction from nanowires can also be achieved by introducing gradual tapering into the nanowires [33–35]. Directional light extraction from nanowires has been extensively investigated in the context of single photon emitters, and has the potential to increase the V_{oc} from nanowire solar cells. High V_{oc} in nanowire array solar cells compared to their bulk counterparts has been predicted using numerical calculations [36,37], and also experimentally observed in case of InP nanowire array solar cells [2].

Using nanowire arrays for solar cells increases the free surface area and reduces the bulk volume of the solar cell significantly. Surface state assisted non-radiative recombination is a serious issue for nanowires, especially for GaAs because of its large surface recombination velocity. But very good surface passivation can be achieved using chemical methods or by growing a larger bandgap shell around the nanowires, as will be discussed in section 5. Assuming good surface passivation, nanowire arrays reduce the bulk non-radiative recombination in the solar cell and hence the reverse saturation current density by a factor equal to the volume fill fraction of the array, without compromising the absorption of incident light. Reduction in the dark current density without limiting incident light absorption also has advantages for achieving high V_{oc} from the nanowire array solar cells, as can be seen from Eq. (6) (light generated current varies as F_s and the dark current varies as F_{co}).

Numerical calculations indicate that the efficiency of a nanowire array solar cell can reach ~42% (32.5%) for bandgap ~1.43 eV (1.34 eV) under AM 1.5 solar spectrum, and exceed that of a planar, bulk solar cell [32,34] with the same bandgap under similar illumination. The efficiency gain is due to increase in V_{oc} as a consequence of inherent light concentration ability and directional emission of the nanowire array. As discussed earlier, the light concentration ability of the array is equivalent to reducing the reverse saturation current without compromising light absorption, and directional emission is equivalent to reducing the mismatch between absorption and emission solid angles from the nanowire array.

The behavior of V_{oc} in single nanowires that we have discussed using the detailed balance approach, can also be understood using the entropic loss approach [Eq. (7)]. The light generated current in the solar cell and the dark current are related to Ω_{sun} and Ω_{em} , respectively. The open circuit voltage from the solar cell varies as the log of the ratio of the light generated current and the dark current [Eq. (6)], and can be increased by increasing Ω_{sun} or reducing Ω_{em} . Light concentration effect that gives rise to excellent light absorption properties of the nanowires is equivalent to increasing the solid angle of absorption Ω_{sun} . The directional emission from nanowires is equivalent to reducing Ω_{em} . This reduces the entropy term associated with reduction in V_{oc} (third term on the right hand side of Eq. (7) and leads to higher V_{oc} in the solar cell.

Since both J_{sc} and V_{oc} of single nanowire solar cells are higher than those in an equivalent volume planar solar cell with the same absorber, single nanowire solar cells have higher efficiencies compared to planar solar cells of equivalent volume. As discussed earlier, both J_{sc} and V_{oc} show oscillations with nanowire diameter. Hence the ultimate efficiency of a single nanowire solar cell is also a function of physical dimensions of the nanowire, not just its bandgap. The ultimate efficiency for a nanowire array solar cell is also higher than a planar

Optics EXPRESS

solar cell. In this case, the efficiency advantage comes from higher V_{oc}. The maximum J_{sc} is the same as in a planar solar cell, although this current density can be achieved with lower volume absorber material.

4. Electrical design

In addition to the theoretical ultimate efficiency advantage for nanowire solar cells discussed in section 3, the junction configuration in the nanowires may also have advantages for photogenerated carrier separation and collection. The device physics of nanowire solar cells was first studied by Brendan Kayes et. al. [1]. The performance characteristics (short circuit current density, open circuit voltage, fill-factor and efficiency) of a nanowire solar cell with radial p-n junctions in each nanowire were compared to that of a planar, bulk solar cell with the same active material and thickness equal to the length/height of the nanowire array. The analytical model presented allows to study the effect of material quality (minority carrier diffusion length) and structural parameters of the nanowire array on the performance of a nanowire solar cell, and compare it to the characteristics of a bulk, planar solar cell.

The outcomes of the model suggest that the nanowire geometry is beneficial for photogenerated carrier collection in solar cells when the minority carrier diffusion length in the active material is much smaller than the thickness required to absorb a significant portion of the incident solar spectrum. Under these conditions, radial junction nanowire solar cells present superior performance characteristics due to their ability to decouple the optical thickness of the solar cell from its electrical thickness. However, in order to take advantage of the ability of radial junction nanowires to decouple the optical and electrical thickness of the solar cell, the trap level or the recombination in the depletion region of the p-n junction in the nanowires should be minimized. For direct bandgap semiconductors like GaAs and InP, the optical thickness required for efficient absorption of incident solar spectrum is of the order of few 100s of nms. Minority carrier diffusion lengths of the order of few 100 nms are routinely achieved for epitaxial III-V semiconductors. Hence, radial junction nanowire solar cells may not present any advantages over their bulk counterparts in terms of photogenerated carrier collection abilities for epitaxial III-V semiconductors.

While the above discussed model takes into account surface recombination, free carrier absorption and junction recombination, it does not account for the light trapping properties of nanowires. Light absorption in nanowires was assumed to be similar to bulk material of equivalent thickness. Analytical model that takes into account the light trapping ability of nanowire arrays was later developed in 2011 [38], and the main outcomes of the study essentially re-iterated that the nanowire configuration for solar cells has advantages in terms of enhanced photo-generated carrier collection efficiencies only for materials with low minority carrier diffusion lengths compared to the required optical thickness, and only when the recombination in the depletion region of the p-n junction can be minimized.

An analysis of the effect of contacting approach on the performance characteristics of a radial p-n junction nanowire array solar cell was later developed [39]. The study focused on GaAs nanowires, considering its large surface recombination velocity (~10^6 cm/s) and existence of near midgap Fermi level pinning due to charge traps created at GaAs/metal interface. The study illustrates that in order to achieve high power conversion efficiencies in GaAs radial p-n junction nanowire array solar cells, the nanowire sidewalls should be passivated to eliminate surface charge traps and the nanowires should be contacted on the tip. With contacts on the sidewalls of the nanowires, the power conversion efficiency of the nanowire array solar cell is drastically reduced due to surface depletion in the nanowire.

None of the above studies take into account the non-uniform carrier generation profiles that result from light trapping in nanowire arrays. While these models provide an understanding of the effect of material and junction quality on the performance of nanowire array solar cells, the actual carrier generation profile should be considered for optimizing the design of nanowire array solar cells [40].

5. Challenges

While the inherent light concentration ability of nanowires potentially promises high power conversion efficiencies through the physical phenomena discussed in sections 2 and 3, the ability to realize these promised efficiencies in a practical device are reliant on the ability to separate and collect photo-generated electrons and holes through the electrical contacts. Surface state engineering and the ability to achieve controlled doping of nanowires are essential for efficient separation and collection of photo-generated carriers from nanowire solar cells. We will discuss the challenges associated with and the current status of surface passivation and doping of nanowires in this section.

First, we will discuss the issues arising due to surface states and the progress made to minimize surface state effects in nanowires. The surface states in semiconductor nanowires influence both optical and electrical properties. Electron/hole traps at the nanowire surface introduce parasitic non-radiative recombination processes and degrade the nanowire device performance. The surface state assisted recombination reduces the non-radiative lifetime of minority carriers in the nanowires. Fermi level pinning due to high density of surface states may deplete the entire nanowire of free charge carriers, severely degrading its electrical properties [41–45]. Surface band bending also affects the ability to form good Ohmic contacts to nanowires, severely degrading the performance of nanowire based devices.

To alleviate these problems it is essential to be able to control the surface state density or surface recombination velocity and doping of nanowires. The surface recombination velocity for InP is three orders of magnitude smaller than the surface recombination velocity of GaAs [46,47], and is not as serious an issue for nanowire devices as it is for GaAs. For this reason most of the published research on engineering nanowire surface states focuses on GaAs rather than InP. The surface state density in compound semiconductors is controlled via surface passivation. Both chemical methods and in situ growth of higher bandgap layers have been used to passivate/control surface state density in III-V semiconductor nanowires. Chemical passivation methods rely on cleaning native oxides from the surface of the semiconductor and forming a thin, chemically inert layer. Sulfur passivation using $Na_2S.9H_2O$ or $(NH_4)_2S_x$ has been used to chemically passivate bulk and nanowire GaAs surfaces [48–53]. A thin layer of GaN can be formed on the GaAs surface through chemical reaction [54,55]. Larger Ga-N bond strength prevents formation of native oxide on the semiconductor surface and reduces surface state density [54]. Chemical treatment in a solution of butanol/HF/trioctylphosphine has been used to passivate InP nanowires [56]. All these chemical approaches have resulted in enhanced photoluminescence and conductivity in nanowires [50,55,56]. While the chemical approaches to reduce the surface state density in nanowires are as effective as in situ growth of larger bandgap materials, surface passivation using chemical approaches only survive for few months under ambient conditions [53,55,57].

‘Surface free’ epitaxial bulk semiconductors are routinely grown using in situ surface passivation. For example, bulk GaAs layers can be made ‘surface free’ by AlGaAs passivation [58]. AlGaAs is lattice matched to GaAs for a wide composition range and its larger bandgap prevents carriers in GaAs from accessing surface states. Long term stable surface passivation can be achieved in GaAs nanowires by growing lattice matched AlGaAs shells around the nanowire core. An AlGaAs shell reduces the surface state/trap density in GaAs nanowires leading to enhanced minority carrier lifetimes, carrier mobilities and diffusion lengths [43,44,59–61]. The surface recombination velocity for bare (unpassivated) GaAs nanowires is ~10^6 cm/s [52]. With AlGaAs passivation, the surface recombination velocity is reduced by three orders of magnitude [43,44], enabling minority carrier lifetimes of the order of 1-3 ns. Lattice matched or strained InGaP can also be used to passivate GaAs surfaces because of its larger bandgap. InGaP shells have been used to passivate GaAs nanowire surfaces, resulting in enhanced luminescence efficiency [62] and higher efficiency GaAs nanowire array solar cells [63]. Lattice mismatched growth of few monolayer thick InP and GaP shells on GaAs nanowires has also been demonstrated as an avenue for passivating

GaAs nanowire surfaces [64]. The observed surface passivation effect in terms of increase in photoluminescence intensity was comparable to that achieved using lattice matched AlGaAs shells around GaAs nanowires.

The conventional approach to separate photo-generated electron-hole pairs in an inorganic solar cell is to use the field gradients generated at a p-n junction. As discussed in section 2, most of the incident light can be absorbed in nanowires with axial dimensions of ~2 μm and lateral dimensions of few 100 nms. Considering the dimensions of nanowires required for efficient light absorption and the depletion region widths, it is essential to be able to control the doping in nanowires very precisely for solar cell applications. Diffusion doping may not be suitable for nanowire solar cells as it results in a less-sharp dopant profile. For this reason, epitaxial growth of doped nanowires is a better option. However, epitaxial growth and doping of nanowires is very different to that of planar epitaxy because of different growth temperatures, growth facets and growth mechanisms and may be an issue for achieving excellent control on doping as is routinely achieved in the case of planar samples.

The first report on growth of doped nanowires was published as early as 1992 [65]. They demonstrated light emission from p-n junctions formed in GaAs nanowires. Following this report, both n- and p-doped bulk GaAs and InP nanowires were grown. Si, Te and Sn were investigated as donors [66–73] and Zn, Be and C were investigated as acceptors for doping bulk GaAs and InP nanowires [69–79]. The amphoteric nature of Si has enabled its use as an acceptor as well in GaAs [80–82]. Both n- and p- doping concentrations as high as $10^{19}/cm^3$ were achieved in GaAs and InP nanowires. However, bulk doping resulted in reduced carrier mobilities in the nanowire due to impurity scattering [83]. It is important to ensure that the immobile ionized donor/acceptor atoms do not compromise the electrical properties of nanowires via impurity scattering. Modulation doping, where dopants or donors/acceptors are not directly incorporated into the core of the nanowire has been predicted to improve the charge transport properties of nanowires [84]. Following these predictions, modulation doping has been investigated as an approach to improve charge carrier concentration without increasing impurity scattering in nanowires. Si modulation doping has been used to increase the electron concentration in GaAs core of AlGaAs passivated nanowires to $\sim 1 \times 10^{16}/cm^3$ [85,86] without degrading the electron mobility compared to undoped nanowires. The effect of Si bulk and modulation doping on the structural morphology of GaAs/AlGaAs nanowires has also been investigated [87].

6. Outlook

From fundamental efficiency limitations point of view, nanowire solar cells have the ability to surpass the efficiency of planar, bulk solar cells. The growth of very good optical quality nanowires and nanowire arrays with control on position and dimensions of nanowires has been achieved by several research groups. The major limiting factor in achieving high efficiencies in nanowire solar cells has been the challenges associated with photogenerated carrier separation and collection phenomenon. Improvements in nanofabrication techniques and the ability to achieve good control on doping the nanowires are required to attain high efficiency nanowire solar cells. Characterisation techniques to analyze the doping and related optoelectronic properties of semiconductors also need to be adapted to suit nanowires. With these developments, nanowire solar cells offer the promise of efficiencies higher than their bulk counterparts, but with smaller active volumes. Alternative solar cell designs that do not require controlled doping in nanowires are also very interesting and promising to overcome the current challenges with achieving high efficiencies in nanowire solar cells. Such designs exploit electron transparent, hole blocking and electron blocking, hole transparent contacts for photogenerated carrier separation instead of relying on electric field gradients generated by doping the nanowires.

Optics EXPRESS

Funding

Australian Research Council (ARC); Australian National Fabrication Facility (ANFF); and National Computational Infrastructure (NCI).

Acknowledgments

The authors acknowledge D. Saxena and Y. Wenas for assistance with figures.